PHYSICAL REVIEW D **77,** 091103(R) (2008)

Measurements of time-dependent CP violation in $B^0 \to \psi(2S)K^0_S$ decays

H. Sahoo,[6] T. E. Browder,[6] K. Trabelsi,[7] I. Adachi,[7] H. Aihara,[40] K. Arinstein,[1] T. Aushev,[11,16] S. Bahinipati,[2] A. M. Bakich,[35] V. Balagura,[11] E. Barberio,[19] A. Bay,[16] I. Bedny,[1] K. Belous,[10] U. Bitenc,[12] A. Bondar,[1] A. Bozek,[25] M. Bračko,[12,18] M.-C. Chang,[3] Y. Chao,[24] A. Chen,[22] W. T. Chen,[22] B. G. Cheon,[5] R. Chistov,[11] I.-S. Cho,[45] Y. Choi,[34] J. Dalseno,[19] M. Dash,[44] A. Drutskoy,[2] S. Eidelman,[1] B. Golob,[12,17] H. Ha,[14] J. Haba,[7] K. Hara,[20] T. Hara,[30] K. Hayasaka,[20] H. Hayashii,[21] M. Hazumi,[7] D. Heffernan,[30] Y. Hoshi,[38] W.-S. Hou,[24] Y. B. Hsiung,[24] H. J. Hyun,[15] K. Inami,[20] A. Ishikawa,[31] H. Ishino,[41] R. Itoh,[7] M. Iwasaki,[40] N. J. Joshi,[36] D. H. Kah,[15] J. H. Kang,[45] P. Kapusta,[25] N. Katayama,[7] H. Kichimi,[7] H. J. Kim,[15] Y. J. Kim,[4] K. Kinoshita,[2] S. Korpar,[12,18] Y. Kozakai,[20] P. Križan,[12,17] P. Krokovny,[7] R. Kumar,[46] C. C. Kuo,[22] Y. Kuroki,[30] Y.-J. Kwon,[45] J. S. Lee,[34] M. J. Lee,[33] S. E. Lee,[33] T. Lesiak,[25] J. Li,[6] A. Limosani,[19] D. Liventsev,[11] F. Mandl,[9] A. Matyja,[25] S. McOnie,[35] T. Medvedeva,[11] W. Mitaroff,[9] K. Miyabayashi,[21] H. Miyake,[30] H. Miyata,[27] Y. Miyazaki,[20] R. Mizuk,[11] G. R. Moloney,[19] E. Nakano,[29] M. Nakao,[7] Z. Natkaniec,[25] S. Nishida,[7] O. Nitoh,[43] S. Noguchi,[21] S. Ogawa,[37] T. Ohshima,[20] S. Okuno,[13] S. L. Olsen,[6,8] P. Pakhlov,[11] G. Pakhlova,[11] H. Palka,[25] C. W. Park,[34] H. Park,[15] L. S. Peak,[35] R. Pestotnik,[12] L. E. Piilonen,[44] Y. Sakai,[7] O. Schneider,[16] C. Schwanda,[9] A. J. Schwartz,[2] K. Senyo,[20] M. E. Sevior,[19] M. Shapkin,[10] C. P. Shen,[8] H. Shibuya,[37] J.-G. Shiu,[24] B. Shwartz,[1] A. Somov,[2] S. Stanič,[28] M. Starič,[12] K. Sumisawa,[7] T. Sumiyoshi,[42] F. Takasaki,[7] M. Tanaka,[7] G. N. Taylor,[19] Y. Teramoto,[29] I. Tikhomirov,[11] S. Uehara,[7] K. Ueno,[24] Y. Unno,[5] S. Uno,[7] P. Urquijo,[19] Y. Usov,[1] G. Varner,[6] K. E. Varvell,[35] K. Vervink,[16] S. Villa,[16] C. H. Wang,[23] P. Wang,[8] X. L. Wang,[8] Y. Watanabe,[13] R. Wedd,[19] E. Won,[14] H. Yamamoto,[39] Y. Yamashita,[26] C. C. Zhang,[8] Z. P. Zhang,[32] V. Zhulanov,[1] and A. Zupanc[12]

(Belle Collaboration)

[1]*Budker Institute of Nuclear Physics, Novosibirsk*
[2]*University of Cincinnati, Cincinnati, Ohio 45221*
[3]*Department of Physics, Fu Jen Catholic University, Taipei*
[4]*The Graduate University for Advanced Studies, Hayama*
[5]*Hanyang University, Seoul*
[6]*University of Hawaii, Honolulu, Hawaii 96822*
[7]*High Energy Accelerator Research Organization (KEK), Tsukuba*
[8]*Institute of High Energy Physics, Chinese Academy of Sciences, Beijing*
[9]*Institute of High Energy Physics, Vienna*
[10]*Institute of High Energy Physics, Protvino*
[11]*Institute for Theoretical and Experimental Physics, Moscow*
[12]*J. Stefan Institute, Ljubljana*
[13]*Kanagawa University, Yokohama*
[14]*Korea University, Seoul*
[15]*Kyungpook National University, Taegu*
[16]*École Polytechnique Fédérale de Lausanne (EPFL), Lausanne*
[17]*Faculty of Mathematics and Physics, University of Ljubljana, Ljubljana*
[18]*University of Maribor, Maribor*
[19]*University of Melbourne, School of Physics, Victoria 3010*
[20]*Nagoya University, Nagoya*
[21]*Nara Women's University, Nara*
[22]*National Central University, Chung-li*
[23]*National United University, Miao Li*
[24]*Department of Physics, National Taiwan University, Taipei*
[25]*H. Niewodniczanski Institute of Nuclear Physics, Krakow*
[26]*Nippon Dental University, Niigata*
[27]*Niigata University, Niigata*
[28]*University of Nova Gorica, Nova Gorica*
[29]*Osaka City University, Osaka*
[30]*Osaka University, Osaka*
[31]*Saga University, Saga*
[32]*University of Science and Technology of China, Hefei*
[33]*Seoul National University, Seoul*
[34]*Sungkyunkwan University, Suwon*

[35]*University of Sydney, Sydney, New South Wales*
[36]*Tata Institute of Fundamental Research, Mumbai*
[37]*Toho University, Funabashi*
[38]*Tohoku Gakuin University, Tagajo*
[39]*Tohoku University, Sendai*
[40]*Department of Physics, University of Tokyo, Tokyo*
[41]*Tokyo Institute of Technology, Tokyo*
[42]*Tokyo Metropolitan University, Tokyo*
[43]*Tokyo University of Agriculture and Technology, Tokyo*
[44]*Virginia Polytechnic Institute and State University, Blacksburg, Virginia 24061*
[45]*Yonsei University, Seoul*
[46]*Panjab University, Chandigarh*

(Received 4 February 2008; published 13 May 2008)

We report improved measurements of time-dependent *CP* violation parameters for $B^0(\bar{B}^0) \to \psi(2S)K^0_S$. This analysis is based on a data sample of 657×10^6 $B\bar{B}$ pairs collected at the $\Upsilon(4S)$ resonance with the Belle detector at the KEKB energy-asymmetric e^+e^- collider. We fully reconstruct one neutral B meson in the $\psi(2S)K^0_S$ *CP*-eigenstate decay channel, and the flavor of the accompanying B meson is identified to be either B^0 or $\bar{B}^0$ from its decay products. *CP* violation parameters are obtained from the asymmetries in the distributions of the proper-time intervals between the two B decays: $\mathcal{S}_{\psi(2S)K^0_S} = +0.72 \pm 0.09(\text{stat}) \pm 0.03(\text{syst})$, $\mathcal{A}_{\psi(2S)K^0_S} = +0.04 \pm 0.07(\text{stat}) \pm 0.05(\text{syst})$. These results are in agreement with results from measurements of $B^0 \to J/\psi K^0$.

DOI: 10.1103/PhysRevD.77.091103 PACS numbers: 11.30.Er, 12.15.Hh, 13.25.Hw

In the standard model, *CP* violation in B^0 meson decays originates from an irreducible complex phase in the 3×3 Cabibbo-Kobayashi-Maskawa (CKM) mixing matrix [1]. In the decay chain $\Upsilon(4S) \to B^0\bar{B}^0 \to f_{CP}f_{\text{tag}}$, where one of the B mesons decays at time t_{CP} to a *CP* eigenstate f_{CP} and the other decays at time t_{tag} to a final state f_{tag} that distinguishes between B^0 and $\bar{B}^0$, the decay rate has a time dependence [2] given by

$$\mathcal{P}(\Delta t) = \frac{e^{-|\Delta t|/\tau_{B^0}}}{4\tau_{B^0}}\{1 + q \cdot [\mathcal{S}_{f_{CP}} \sin(\Delta m_d \Delta t) + \mathcal{A}_{f_{CP}} \cos(\Delta m_d \Delta t)]\}. \quad (1)$$

Here $\mathcal{S}_{f_{CP}}$ and $\mathcal{A}_{f_{CP}}$ are the *CP* violation parameters, τ_{B^0} is the neutral B lifetime, Δm_d is the mass difference between the two neutral B mass eigenstates, $\Delta t = t_{CP} - t_{\text{tag}}$, and the b-flavor charge q equals $+1$ (-1) when the tagging B meson is a B^0 $(\bar{B}^0)$. For f_{CP} final states resulting from a $b \to c\bar{c}s$ transition, the standard model predicts $\mathcal{S}_{f_{CP}} = -\xi_f \sin 2\phi_1$ [3] and $\mathcal{A}_{f_{CP}} \simeq 0$, where $\xi_f = +1$ (-1) for *CP*-even (*CP*-odd) final states and ϕ_1 is one of the three interior angles of the CKM unitarity triangle, defined as $\phi_1 \equiv \pi - \arg(V^*_{tb}V_{td}/V^*_{cb}V_{cd})$. Measurements of *CP* asymmetries in $b \to c\bar{c}s$ transitions have been reported by Belle [4,5] and *BABAR* [6]. Results from our previously published $B^0 \to \psi(2S)K^0_S$ analysis were based on a 140 fb^{-1} data sample corresponding to 152×10^6 $B\bar{B}$ pairs [4]. Here we report new measurements with an improved analysis [7] incorporating an additional 465 fb^{-1} data sample for a total of 605 fb^{-1} (657×10^6 $B\bar{B}$ pairs).

At the KEKB energy-asymmetric e^+e^- (3.5 on 8.0 GeV) collider [8], the $\Upsilon(4S)$ is produced with a Lorentz boost of $\beta\gamma = 0.425$ nearly along the z axis, which is defined as opposite to the positron beam direction. Since the B^0 and $\bar{B}^0$ are approximately at rest in the $\Upsilon(4S)$ center-of-mass system (cms), Δt can be determined from the displacement in z between the two decay vertices: $\Delta t \simeq \Delta z/(\beta\gamma c)$, where c is the speed of light.

The Belle detector is a large-solid-angle magnetic spectrometer that consists of a silicon vertex detector (SVD), a 50-layer central drift chamber (CDC), an array of aerogel threshold Cherenkov counters (ACC), a barrel-like arrangement of time-of-flight scintillation counters (TOF), and an electromagnetic calorimeter (ECL) comprised of CsI(Tl) crystals located inside a superconducting solenoid coil that provides a 1.5 T magnetic field. An iron flux-return located outside the coil is instrumented to detect K^0_L mesons and to identify muons (KLM). The detector is described in detail elsewhere [9]. Two different inner detector configurations were used. For the first sample of 152×10^6 $B\bar{B}$ pairs, a 2.0 cm radius beampipe and a 3-layer silicon vertex detector (SVD-I) were used; for the latter 505×10^6 $B\bar{B}$ pairs, a 1.5 cm radius beampipe, a 4-layer silicon detector (SVD-II), and a small-cell inner drift chamber were used [10].

We reconstruct $\psi(2S)$ mesons in the l^+l^- decay channel ($l = e$ or μ) and $J/\psi\pi^+\pi^-$ decay channel. J/ψ mesons are reconstructed in the l^+l^- decay channel and include the bremsstrahlung photons that are within 50 mrad of each of the e^+ and e^- tracks [denoted as $e^+e^-(\gamma)$]. The invariant mass of the J/ψ candidates is required to be within $-0.150\ \text{GeV}/c^2 < M_{e^+e^-(\gamma)} - m_{J/\psi} < +0.036\ \text{GeV}/c^2$ and $-0.060\ \text{GeV}/c^2 < M_{\mu^+\mu^-} - m_{J/\psi} < +0.036\ \text{GeV}/c^2$, where $m_{J/\psi}$ denotes the world-average J/ψ mass [11],

and $M_{e^+e^-(\gamma)}$ and $M_{\mu^+\mu^-}$ are the reconstructed invariant masses of the $e^+e^-(\gamma)$ and $\mu^+\mu^-$ candidates, respectively. For the $\psi(2S) \to l^+l^-$ candidates, the same procedure is used. In this case, the invariant mass is required to be within $-0.150\ \mathrm{GeV}/c^2 < M_{e^+e^-(\gamma)} - m_{\psi(2S)} < +0.036\ \mathrm{GeV}/c^2$ and $-0.060\ \mathrm{GeV}/c^2 < M_{\mu^+\mu^-} - m_{\psi(2S)} < +0.036\ \mathrm{GeV}/c^2$, where $m_{\psi(2S)}$ denotes the world-average $\psi(2S)$ mass [11]. For the $\psi(2S) \to J/\psi\pi^+\pi^-$ candidates, $\Delta M \equiv M_{l^+l^-\pi^+\pi^-} - M_{l^+l^-}$ is required to be within $0.580\,\mathrm{GeV}/c^2 < \Delta M < 0.600\,\mathrm{GeV}/c^2$. To reduce the fraction of incorrectly reconstructed $\psi(2S)$ signal candidates, we select $\pi^+\pi^-$ pairs with an invariant mass greater than 400 MeV/c^2. The K^0_S selection criteria are the same as those described in Ref. [12]; the invariant mass of the pion pairs is required to satisfy $0.482\ \mathrm{GeV}/c^2 < M_{\pi^+\pi^-} < 0.514\ \mathrm{GeV}/c^2$.

We combine the $\psi(2S)$ and K^0_S to form a neutral B meson. The B candidates are identified using two kinematic variables: the energy difference $\Delta E \equiv E_B^{\mathrm{cms}} - E_{\mathrm{beam}}^{\mathrm{cms}}$ and the beam-energy-constrained mass $M_{\mathrm{bc}} \equiv \sqrt{(E_{\mathrm{beam}}^{\mathrm{cms}})^2 - (p_B^{\mathrm{cms}})^2}$, where $E_{\mathrm{beam}}^{\mathrm{cms}}$ is the beam energy in the cms, and E_B^{cms} and p_B^{cms} are the cms energy and momentum, respectively, of the reconstructed B candidate. In order to improve the ΔE resolution, the masses of the selected J/ψ and $\psi(2S)$ candidates are constrained to their nominal masses using mass-constrained kinematic fits. For the CP asymmetry fit, we select the candidates in the ΔE-M_{bc} signal region defined as $|\Delta E| < 0.03$ GeV and $5.27\ \mathrm{GeV}/c^2 < M_{\mathrm{bc}} < 5.29\ \mathrm{GeV}/c^2$. To suppress background from $e^+e^- \to q\bar{q}$ ($q = u, d, s$, or c) continuum events, we require that the event-shape variable R_2 be less than 0.5, where R_2 is the ratio of second to zeroth Fox-Wolfram moments [13].

The b flavor of the accompanying B meson is identified by a tagging algorithm [14] that categorizes charged leptons, kaons, and Λ baryons found in the event. The algorithm returns two parameters: the b-flavor charge q, and r, which measures the tag quality and varies from $r = 0$ for no flavor discrimination to $r = 1$ for unambiguous flavor assignment. If $r < 0.1$, the accompanying B meson provides negligible tagging information and we set the wrong tag probability to 0.5. Events with $r > 0.1$ are divided into six r intervals.

The vertex position for the f_{CP} decay is reconstructed using charged tracks that have a minimum number of SVD hits [15]. A constraint on the interaction point is also used with the selected tracks; the interaction point profile is convolved with the finite B-flight length in the plane perpendicular to the z axis. The pions from K^0_S decays are not used for vertexing. The typical vertex reconstruction efficiency and z resolution are 95% and 78 μm, respectively [12]. The f_{tag} vertex determination is obtained with well-reconstructed tracks that are not assigned to f_{CP}. The typical vertex reconstruction efficiency and z resolution are 93% and 140 μm, respectively [12]. After all selection criteria are applied, we obtain 1618 and 1202 events for the l^+l^- and $J/\psi\pi^+\pi^-$ modes in the ΔE-M_{bc} fit region defined as $5.2\ \mathrm{GeV}/c^2 < M_{\mathrm{bc}} < 5.3\ \mathrm{GeV}/c^2$ and $-0.1\ \mathrm{GeV} < \Delta E < 0.1\ \mathrm{GeV}$, of which 680 and 712, respectively, are in the signal region.

Figure 1 shows the reconstructed variables ΔE and M_{bc} after flavor tagging and vertex reconstruction. The signal yield is obtained from an extended unbinned maximum-likelihood fit to the ΔE-M_{bc} distribution. We model the shape for the signal component using the product of a double Gaussian for ΔE and a single Gaussian for M_{bc}, whereas the combinatorial background is described by the product of a first-order polynomial for ΔE and an ARGUS [16] function for M_{bc}. For the $\psi(2S) \to J/\psi\pi^+\pi^-$ mode, there is a background component that peaks like the signal (peaking background) in the ΔE-M_{bc} signal region. This peaking background is mainly due to the $J/\psi K_1(1270)^0$, $J/\psi K^*(892)^-\pi^+$, and $J/\psi K^0_S\pi^+\pi^-$ modes, with no real

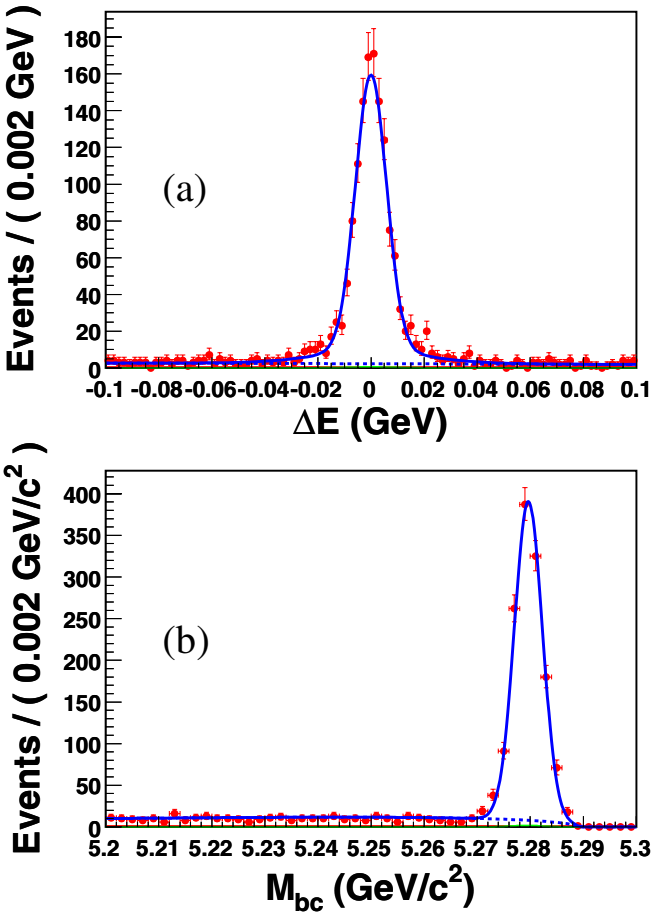

FIG. 1 (color online). (a) ΔE distribution within the M_{bc} signal region, (b) M_{bc} distribution within the ΔE signal region for $B^0 \to \psi(2S)K^0_S$. The solid curves show the fits to the signal plus background distributions, while the dashed curves show the background contributions. The small contribution from peaking backgrounds is discussed in the text.

TABLE I. Number of signal B candidates (N_{sig}) and estimated purity (p) in the signal region after flavor tagging and vertex reconstruction.

Mode	N_{sig}	p
$\psi(2S)(l^+l^-)K^0_S$	628 ± 26	0.92 ± 0.01
$\psi(2S)(J/\psi\pi^+\pi^-)K^0_S$	656 ± 26	0.92 ± 0.01

$\psi(2S) \to J/\psi\pi^+\pi^-$ in the final state. The fraction of such peaking events is estimated to be 1% from the ΔM sidebands in data. The signal and background shapes for each decay mode are determined from Monte Carlo (MC) events; these shapes are adjusted for small differences between MC and data using a control sample of $B^+ \to \psi(2S)K^+$ [17] events, which have a final state similar to the signal but with higher statistics. This sample, where no CP asymmetry is expected, is also used to check the potential bias in the measurements of CP violation parameters. The signal yields and purity in the ΔE-M_{bc} signal region after flavor tagging and vertex reconstruction are listed in Table I. We define the purity as the ratio of the signal yield to the total number of candidate events in the signal region.

We determine $\mathcal{S}_{f_{CP}}$ and $\mathcal{A}_{f_{CP}}$ by performing an unbinned maximum-likelihood fit to the observed Δt distribution for the candidate events in the signal region. The likelihood function is

$$\mathcal{L}(\mathcal{S}_{f_{CP}}, \mathcal{A}_{f_{CP}}) = \prod_i \mathcal{P}_i(\mathcal{S}_{f_{CP}}, \mathcal{A}_{f_{CP}}; \Delta t_i), \qquad (2)$$

where the product includes events in the signal region. We only use events with vertices that satisfy $|\Delta t| < 70$ ps and $\xi < 250$, where ξ is the χ^2 of the vertex fit calculated only in the z direction. The probability density function (PDF) is given by

$$\begin{aligned}\mathcal{P}_i = (1 - f_{ol}) \int [& f_{sig}\mathcal{P}_{sig}(\Delta t')R_{sig}(\Delta t_i - \Delta t') \\ & + f_{peak}\mathcal{P}_{peak}(\Delta t')R_{sig}(\Delta t_i - \Delta t') \\ & + (1 - f_{sig} - f_{peak})\mathcal{P}_{bkg}(\Delta t')R_{bkg}(\Delta t_i - \Delta t')]d(\Delta t') \\ & + f_{ol}P_{ol}(\Delta t_i). \end{aligned} \qquad (3)$$

The signal fraction f_{sig} and the peaking fraction f_{peak} depend on the r region and are calculated on an event-by-event basis as a function of ΔE and M_{bc}. The PDF for signal events, $\mathcal{P}_{sig}(\Delta t)$, is given by Eq. (1) and modified to incorporate the effect of incorrect flavor assignment; the parameters τ_{B^0} and Δm_d are fixed to their world-average values [11]. The distribution is then convolved with a resolution function $R_{sig}(\Delta t)$ to take into account the finite vertex resolution. The resolution function parameters, along with the wrong tag fractions for the six r intervals, w_l ($l = 1, 6$), and possible differences in w_l between B^0 and $\bar{B}^0$ decays (Δw_l) are determined using a high-statistics control sample of semileptonic and hadronic $b \to c$ decays [4,12]. The PDF for non-peaking background events, $\mathcal{P}_{bkg}(\Delta t)$, is modeled as a sum of exponential and prompt components and is convolved with a sum of two Gaussians, which parameterizes the resolution function $R_{bkg}(\Delta t)$. Parameters in $\mathcal{P}_{bkg}(\Delta t)$ and $R_{bkg}(\Delta t)$ are determined from a fit to the Δt distribution of events in the ΔE-M_{bc} data sideband ($M_{bc} < 5.26$ GeV/c^2, -0.03 GeV $< \Delta E <$ 0.20 GeV). The PDF for peaking background events, $\mathcal{P}_{peak}(\Delta t)$, is the same as $\mathcal{P}_{sig}(\Delta t)$ with CP parameters fixed to zero. The term $P_{ol}(\Delta t)$ is a broad Gaussian function that represents an outlier component with a small fraction f_{ol}. The only free parameters in the final fit are $\mathcal{S}_{f_{CP}}$ and $\mathcal{A}_{f_{CP}}$; these are determined by maximizing the likelihood function given by Eq. (2).

The unbinned maximum-likelihood fit to the 1300 events in the signal region results in the CP violation parameters,

$$\mathcal{S}_{\psi(2S)K^0_S} = +0.72 \pm 0.09(\text{stat}) \pm 0.03(\text{syst}),$$
$$\mathcal{A}_{\psi(2S)K^0_S} = +0.04 \pm 0.07(\text{stat}) \pm 0.05(\text{syst}),$$

where the systematic uncertainties listed are described below. We define the raw asymmetry in each Δt bin by $(N_+ - N_-)/(N_+ + N_-)$, where N_+ (N_-) is the number of observed candidates with $q = +1$ (-1). Figure 2 shows the observed Δt distributions for $q = +1$ and $q = -1$ with no requirement on the tagging quality (top), and the raw asymmetry for events with good tagging quality ($r > 0.5$) (bottom).

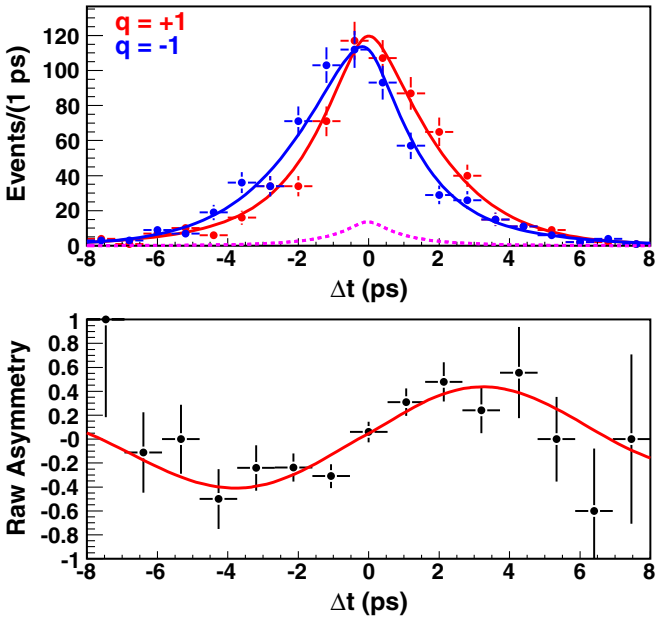

FIG. 2 (color online). The top plot shows the Δt distributions for $q = +1$ and $q = -1$ with no requirement on r. The dashed curve is the sum of backgrounds, while the solid curves are the sum of signal and backgrounds. The bottom plot is the raw asymmetry of well-tagged events ($r > 0.5$, 45% of the total). The solid curve shows the result of the unbinned maximum-likelihood fit.

The systematic errors on $\mathcal{S}_{f_{CP}}$ and $\mathcal{A}_{f_{CP}}$, summarized in Table II, are evaluated by fitting the data with each fixed parameter varied by its 1 standard deviation (σ) error. The MC-determined parameters are varied by $\pm 2\sigma$ to take into account possible imperfect modeling in the MC. We repeat the *CP* fit procedure with the new value, add the differences in S, A quadratically, and then assign the result as the systematic error. The largest contribution to $\mathcal{S}_{f_{CP}}$ comes from vertex reconstruction (0.026). This includes the uncertainties in the interaction point profile (the smearing used to account for the B flight length is varied by -10μm and $+20\mu$m), the tag side track selection criteria, the helix parameter correction, the $|\Delta t|$ range (varied by ± 30 ps), the vertex quality cut ξ (changed to $\xi < 150$ and $\xi < 500$), the Δz measurement, and imperfect SVD alignment. The last two are obtained from a study of $J/\psi K^0_S$. Each physics parameter (τ_{B^0}, Δm_d) is varied by the error in its world-average value [11]. Systematic errors due to uncertainties in wrong tag fractions are estimated by varying the parameters w_l, Δw_l in each r region by their $\pm 1\sigma$ errors. Systematic errors due to uncertainties in the resolution function are estimated by varying each resolution parameter obtained from data (MC) by $\pm 1\sigma$ ($\pm 2\sigma$). The ΔE, $M_{\rm bc}$ parameters and signal fraction in each r region are varied to estimate the systematic errors. No significant bias is seen by fitting a large sample of MC events. The systematic errors from uncertainties in the peaking background are obtained by varying the peaking fraction, shape, as well as its *CP* asymmetry parameters. The systematic errors from uncertainties in the background Δt shape are estimated by varying each background parameter by its statistical error. We also include the effects of interference between CKM-favored and CKM-suppressed $B \to D$ transitions in the $f_{\rm tag}$ final state [18]. We add each contribution above in quadrature to obtain the total systematic uncertainty.

We perform various cross-checks for this measurement. A fit to the first data sample (SVD-I) results in the *CP* violation parameter, $\mathcal{S} = 0.97 \pm 0.18$, which is consistent with our previous result [4]. A fit to the *CP* asymmetries of the control sample gives the *CP* violation parameters, $\mathcal{S} = 0.02 \pm 0.05$ and $\mathcal{A} = -0.03 \pm 0.03$, which are consistent with no *CP* asymmetry. A fit to the sideband events in the $B^0 \to \psi(2S)K^0_S$ data sample gives an asymmetry consistent with zero ($\mathcal{S} = 0.02 \pm 0.21$, $\mathcal{A} = -0.04 \pm 0.10$). A lifetime fit to $B^0 \to \psi(2S)K^0_S$ and $B^+ \to \psi(2S)K^+$ gives $\tau_{B^0} = 1.51 \pm 0.05$ ps and $\tau_{B^+} = 1.62 \pm 0.03$ ps, respectively, which are consistent with the world-average values. We also examine the *CP* violation parameters separately for the $\psi(2S) \to l^+l^-$ ($\mathcal{S} = 0.84 \pm 0.13$, $\mathcal{A} = 0.14 \pm 0.09$) and $\psi(2S) \to J/\psi\pi^+\pi^-$ ($\mathcal{S} = 0.61 \pm 0.13$, $\mathcal{A} = -0.09 \pm 0.10$) decay modes. We find that all results are consistent within errors.

TABLE II. Systematic uncertainties.

Parameter	$\Delta\mathcal{S}_{\psi(2S)K^0_S}$	$\Delta\mathcal{A}_{\psi(2S)K^0_S}$
Vertexing	0.026	0.028
Wrong tag fraction	0.006	0.023
Resolution function	0.007	0.005
Fit bias	0.012	0.011
Physics parameters	0.001	0.001
Peaking background	0.006	0.005
PDF shape and fraction	0.001	0.003
Background Δt shape	0.003	0.003
Tag side interference	0.001	0.036
Total	0.031	0.053

In summary, we have performed improved measurements of *CP* violation parameters $\sin 2\phi_1$ and $\mathcal{A}_{f_{CP}}$ for $B^0 \to \psi(2S)K^0_S$ using 657×10^6 $B\bar{B}$ events. These measurements supersede our previous result [4] and are in agreement with results from measurements of $B^0 \to J/\psi K^0$ [19]. Combining the results from $B^0 \to J/\psi K^0$ [5] and $B^0 \to \psi(2S)K^0_S$ decays, we obtain a new Belle average $\sin 2\phi_1 = 0.650 \pm 0.029 \pm 0.018$.

We thank the KEKB group for excellent operation of the accelerator, the KEK cryogenics group for efficient solenoid operations, and the KEK computer group and the NII for valuable computing and Super-SINET network support. We acknowledge support from MEXT and JSPS (Japan); ARC and DEST (Australia); NSFC (China); DST (India); MOEHRD, KOSEF, and KRF (Korea); KBN (Poland); MES and RFAAE (Russia); ARRS (Slovenia); SNSF (Switzerland); NSC and MOE (Taiwan); and DOE (USA).

[1] N. Cabibbo, Phys. Rev. Lett. **10**, 531 (1963); M. Kobayashi and T. Maskawa, Prog. Theor. Phys. **49**, 652 (1973).

[2] A. B. Carter and A. I. Sanda, Phys. Rev. D **23**, 1567 (1981); I. I. Bigi and A. I. Sanda, Nucl. Phys. **B193**, 85 (1981).

[3] Another naming convention, $\beta(=\phi_1)$, is also used in the literature.

[4] K. Abe *et al.* (Belle Collaboration), Phys. Rev. D **71**, 072003 (2005).

[5] K-F. Chen *et al.* (Belle Collaboration), Phys. Rev. Lett. **98**, 031802 (2007).

[6] B. Aubert *et al.* (*BABAR* Collaboration), Phys. Rev. Lett. **99**, 171803 (2007).

[7] This analysis is improved compared to our previous publication [4]. The peaking backgrounds are estimated directly from the data sidebands. The signal and peaking fraction in the time-dependent PDF are determined for each r bin. In addition to the lepton tracks from the J/ψ, we use the prompt $\pi^+\pi^-$ tracks in the vertex reconstruction for the $\psi(2S)(J/\psi\pi^+\pi^-)K^0_S$ decay mode. Only lepton tracks from the J/ψ were used in the previous analysis.

[8] S. Kurokawa and E. Kikutani, Nucl. Instrum. Methods Phys. Res., Sect. A **499**, 1 (2003), and other papers included in this volume.

[9] A. Abashian *et al.* (Belle Collaboration), Nucl. Instrum. Methods Phys. Res., Sect. A **479**, 117 (2002).

[10] Z. Natkaniec (Belle SVD2 Group), Nucl. Instrum. Methods Phys. Res., Sect. A **560**, 1 (2006).

[11] W.-M. Yao *et al.*, J. Phys. G **33**, 1 (2006).

[12] K-F. Chen *et al.* (Belle Collaboration), Phys. Rev. D **72**, 012004 (2005).

[13] G. C. Fox and S. Wolfram, Phys. Rev. Lett. **41**, 1581 (1978).

[14] H. Kakuno *et al.*, Nucl. Instrum. Methods Phys. Res., Sect. A **533**, 516 (2004).

[15] H. Tajima *et al.*, Nucl. Instrum. Methods Phys. Res., Sect. A **533**, 370 (2004).

[16] H. Albrecht *et al.* (ARGUS Collaboration), Phys. Lett. B **241**, 278 (1990).

[17] Throughout this paper, the inclusion of the charge-conjugate decay mode is implied unless otherwise stated.

[18] O. Long, M. Baak, R. N. Cahn, and D. Kirkby, Phys. Rev. D **68**, 034010 (2003).

[19] See http://www.slac.stanford.edu/xorg/hfag/ for updated results.